



Proton decay and axion dark matter in $SO(10)$ grand unification via minimal left–right symmetry

Yuta Hamada^{1,a}, Masahiro Ibe^{2,3,b}, Yu Muramatsu^{4,c}, Kin-ya Oda^{5,d} , Norimi Yokozaki^{6,e}

¹ Université de Paris, CNRS, Astroparticule et Cosmologie, 75013 Paris, France

² ICRR, University of Tokyo, Kashiwa, Chiba 277-8582, Japan

³ Kavli IPMU (WPI), UTIAS, The University of Tokyo, Kashiwa, Chiba 277-8583, Japan

⁴ Institute of Particle Physics and Key Laboratory of Quark and Lepton Physics (MOE), Central China Normal University, Wuhan 430079, Hubei, People's Republic of China

⁵ Department of Physics, Osaka University, Osaka 560-0043, Japan

⁶ Department of Physics, Tohoku University, Sendai, Miyagi 980-8578, Japan

Received: 31 January 2020 / Accepted: 14 April 2020 / Published online: 28 May 2020
© The Author(s) 2020

Abstract We study the proton lifetime in the $SO(10)$ Grand Unified Theory (GUT), which has the left–right (LR) symmetric gauge theory below the GUT scale. In particular, we focus on the minimal model without the bi-doublet Higgs field in the LR symmetric model, which predicts the LR-breaking scale at around 10^{10-12} GeV. The Wilson coefficients of the proton decay operators turn out to be considerably larger than those in the minimal $SU(5)$ GUT model especially when the Standard Model Yukawa interactions are generated by integrating out extra vector-like multiplets. As a result, we find that the proton lifetime can be within the reach of the Hyper-Kamiokande experiment even when the GUT gauge-boson mass is in the 10^{16-17} GeV range. We also show that the mass of the extra vector-like multiplets can be generated by the Peccei–Quinn symmetry breaking in a consistent way with the axion dark matter scenario.

1 Introduction

The Grand Unified Theory (GUT) [1] is one of the most attractive candidates for physics beyond the Standard Model (SM), which provides an explanation of the charge quantization. In particular, the $SO(10)$ gauge group [2, 3] is one of the most attractive candidates for the unification group as it not only unifies all the gauge interactions in the SM but also unifies a generation of the SM fermions into one representation.

Furthermore, it also predicts the existence of the right-handed neutrinos, which naturally explains the light active neutrino masses through the seesaw mechanism [4–8]. This feature is a great advantage over the $SU(5)$ GUT.

Another interesting feature of the $SO(10)$ GUT is that the rank of $SO(10)$ is larger than the SM. Accordingly, the $SO(10)$ GUT allows various symmetry breaking paths to the SM gauge groups, such as the Left–Right (LR) symmetric groups [9–15]. Among these possibilities, the minimal model based on the $SU(3)_C \times SU(2)_L \times SU(2)_R \times U(1)_{B-L}$ gauge group without a bi-doublet of $SU(2)_L \times SU(2)_R$ uniquely predicts an intermediate breaking scale of the LR symmetry to be around 10^{10-12} GeV [16, 17]; see also [18, 19]. This model also gets renewed attention as it can explain the small Higgs quartic coupling constant at a high energy scale while solving the strong CP problem simultaneously [10–15, 20, 21]. In this class of models, all the SM Yukawa interactions are generated by integrating out extra vector-like multiplets at around the LR-breaking scale.

In this paper, we discuss the proton lifetime in this scenario with the simplest possibility of the extra matter content.¹ As we will see, the preferred GUT scale $\lesssim 10^{17}$ GeV is lower than expected in Refs. [16, 17] by a factor a few or so, due to the effects of the extra matter multiplets on the renormalization group running.² We also find that the Wilson coefficients of the proton decay operators are consid-

^a e-mail: hamada@apc.in2p3.fr

^b e-mail: ibe@icrr.u-tokyo.ac.jp

^c e-mail: yumurasub@gmail.com

^d e-mail: odakin@phys.sci.osaka-u.ac.jp (corresponding author)

^e e-mail: yokozaki@tuhep.phys.tohoku.ac.jp

¹ Hall and Harigaya have extensively studied various possibilities of the extra matter contents [20, 21]. In this paper we only study the simplest one among them, which has also been partly discussed in a different context of the axion dark matter scenario [22].

² Recall that the proton decay rate Γ is inversely proportional to the fourth power of the GUT gauge-boson mass M_X , and hence the slight change of M_X significantly affects Γ .

erably larger than those in the minimal $SU(5)$ GUT model due to the larger gauge coupling below the GUT scale as well as the $SU(2)_R$ gauge interaction at the intermediate scale. As a result, the proton decay rate is enhanced and a parameter region consistent with the gauge coupling unification in the 10^{16} – 10^{17} GeV range can be tested by the Hyper-Kamiokande (Hyper-K) experiment. We also discuss a possibility to generate the mass of the extra vector-like multiplet by the Peccei–Quinn (PQ) symmetry breaking in a consistent way with the axion dark matter scenario.

The organization of the paper is as follows. In Sect. 2, we summarize the $SO(10)$ model which has the minimal LR symmetric gauge group at the intermediate stage. In Sect. 3, we discuss the gauge coupling unification in the minimal LR symmetric model. In Sect. 4, we study the proton lifetime. In Sect. 5, we discuss the mass generation of the extra vector-like multiplets by the PQ symmetry breaking. We give a summary of our discussion in the final section.

2 The minimal setup of the $SO(10)$ GUT model

In this paper, we discuss $SO(10)$ GUT with the following chain of symmetry breaking:

$$SO(10) \xrightarrow{M_{GUT}} G_{LR} \equiv SU(3)_C \times SU(2)_L \times SU(2)_R \times U(1)_{B-L} \xrightarrow{M_R} G_{SM} \equiv SU(3)_C \times SU(2)_L \times U(1)_Y. \quad (1)$$

To ensure this chain and subsequent SM symmetry breaking, we introduce an $SO(10)$ adjoint Higgs H_{45} and an $SO(10)$ spinor-representation Higgs H_{16} . H_{16} contains the doublet Higgs bosons of $SU(2)_R$ and $SU(2)_L$, respectively.³ First, the vacuum expectation value (VEV) of H_{45} breaks down the $SO(10)$ symmetry at the GUT scale M_{GUT} .⁴ Second, the VEV of the $SU(2)_R$ doublet Higgs breaks down the LR symmetry at M_R , which we call the LR symmetry breaking scale. In this setup there is no bi-doublet Higgs. Below the LR symmetry breaking scale, the $U(1)_Y$ gauge symmetry in the SM is obtained by

$$Q_Y = \frac{1}{2} Q_{B-L} - T_3^R, \quad (2)$$

where T_3^R is the third generator of $SU(2)_R$. As will be discussed, the typical values of the GUT and the LR symmetry breaking scales are $M_{GUT} = \mathcal{O}(10^{16-17})$ GeV and

³ It should be noted that H_{45} and H_{16} do not contain the bi-doublet Higgs of $SU(2)_R \times SU(2)_L$.

⁴ It is known that, in this minimal setup, the desired $H_{45} \neq 0$ vacuum is unstable at the tree level and that, for quantum corrections to stabilize the potential, at least a quartic coupling in the tree-level potential must be small [23,24].

$M_R = \mathcal{O}(10^{10-12})$ GeV, respectively. Throughout this paper, we assume these minimal contents for the Higgs sector, and assume that only the doublet Higgs bosons of $SU(2)_R$ and $SU(2)_L$ remain massless below the GUT scale.

In the minimal $SO(10)$ GUT model, each generation of the quarks and the leptons of the SM forms an $SO(10)$ -spinor F_{16} , which is decomposed into the G_{LR} and G_{SM} representations as

$$F_{16} \xrightarrow{M_{GUT}} Q_L(3, 2, 1)_{\frac{1}{3}} + Q_R^c(\bar{3}, 1, 2)_{-\frac{1}{3}} + L_L(1, 2, 1)_{-1} + L_R^c(1, 1, 2)_1 \xrightarrow{M_R} q_L(3, 2)_{\frac{1}{6}} + \left(d_R^c(\bar{3}, 1)_{\frac{1}{3}} + u_R^c(\bar{3}, 1)_{-\frac{2}{3}} \right) + l_L(1, 2)_{-\frac{1}{2}} + \left(e_R^c(1, 1)_1 + \nu_R^c(1, 1)_0 \right), \quad (3)$$

where the subscript is for the charges of B – L and Y , respectively. To embed $U(1)_{B-L}$ into $SO(10)$, we renormalize the charges so that the $U(1)$ gauge couplings are given by⁵

$$\alpha_Y = \frac{3}{5} \alpha_1 \quad (\text{below } M_R), \quad \alpha_{B-L} = \frac{3}{8} \alpha_1 \quad (\text{above } M_R). \quad (4)$$

In the LR symmetric model with only $SU(2)_{L,R}$ doublet Higgs bosons, the Yukawa interactions in the SM are given by the higher-dimensional operators in Table 1. In the $SO(10)$ notation, they correspond to

$$\mathcal{L}_Y = \frac{y_{u ij}}{\Lambda} (F_{16i} H_{16}^*) (F_{16j} H_{16}^*) + \frac{y_{d ij}}{\Lambda} (F_{16i} H_{16}) (F_{16j} H_{16}) + \text{h.c.}, \quad (5)$$

where $i, j = 1, 2, 3$ is the flavor index. Λ is the cutoff scale. Hereafter, we suppress the gauge and the flavor indices unless otherwise stated. After the LR symmetry breaking, these operators contribute to the Yukawa interactions: y_u contributes to the up-type and neutrino ones, while y_d to the down-type and charged-lepton ones. In Table 1, the second and the third columns represent the Yukawa interactions from the higher-dimensional operators in Eq. (5) in the representations of G_{LR} and G_{SM} , respectively.

Obviously, these contributions are too small to realize the observed masses of the heavy flavor fermions in the SM for $\Lambda = M_{GUT}$, for example. In fact, since the LR symmetry breaking scale M_R is around 10^{10} – 10^{11} GeV, while $M_{GUT} = 10^{16}$ – 10^{17} GeV, the coefficient of these operators are $\sim M_R/\Lambda = 10^{-7}$ – 10^{-5} , and hence we cannot realize the Yukawa couplings for the second and third generations. To reproduce the observed quark and lepton masses, we need to introduce extra vector-like multiplets with masses of M_R

⁵ With these normalizations, the Dynkin index of the $U(1)$ gauge group of F_{16} becomes 2.

Table 1 The Yukawa interactions which come from the higher-dimensional operators in Eq. (5)

	G_{LR}	G_{SM}
Up-type Yukawa	$y_u \frac{(Q_R^c H_R^*)(Q_L H_L)}{M_{\text{extra}}}$	$y_u \frac{\langle H_R \rangle}{M_{\text{extra}}} u_R^c (q_L h_L)$
Down-type Yukawa	$y_d \frac{(Q_R^c H_R)(H_L^* Q_L)}{M_{\text{extra}}}$	$y_d \frac{\langle H_R \rangle}{M_{\text{extra}}} d_R^c (h_L^* q_L)$
Charged Lepton Yukawa	$y_d \frac{(L_R^c H_R)(H_L^* L_L)}{M_{\text{extra}}}$	$y_d \frac{\langle H_R \rangle}{M_{\text{extra}}} e_R^c (h_L^* l_L)$
Neutrino Dirac Yukawa	$y_\nu \frac{(L_R^c H_R^*)(L_L H_L)}{M_{\text{extra}}}$	$y_\nu \frac{\langle H_R \rangle}{M_{\text{extra}}} \nu_R^c (l_L h_L)$
Neutrino Majorana mass	$y_\nu \frac{(L_R^c H_R^*)(L_R^c H_R^*)}{M_{\text{extra}}}$	$y_\nu \frac{\langle H_R \rangle^2}{M_{\text{extra}}} \nu_R^c \nu_R^c$

so that the terms in Eq. (5) are generated by integrating out those extra multiplets.

In this paper, we assume that all the SM Yukawa interactions are generated by integrating out extra vector-like multiplets. In this case, the minimal extra vector-like fermions consist of three flavors of the fundamental representation of $SO(10)$, E_{10} , and three flavors of the adjoint representation of $SO(10)$, E_{45} .⁶ When the Yukawa interactions of the first generation are provided by the M_{GUT} suppressed operators, two flavors of E_{10} and E_{45} are enough to reproduce the SM Yukawa interactions. As discussed in Sect. 5, however, the three flavor model is advantageous as the masses of the extra vector-like fermions can be interrelated to the PQ symmetry breaking. In what follows, we denote the number of extra particle flavors by N_E .

With these extra matter multiplets, the origin of the Yukawa interactions in Eq. (5) are obtained from the renormalizable interactions,

$$\mathcal{L}_{\text{extra}} = y'_d F_{16} E_{10} H_{16} + y'_u F_{16} E_{45} H_{16}^* + M_{\text{extra}} E_{10} E_{10} + M_{\text{extra}} E_{45} E_{45} + \text{h.c.}, \tag{6}$$

where M_{extra} is the extra particle mass. We assume that the mass parameters for E_{10} and E_{45} are the same for simplicity. E_{10} and E_{45} are decomposed into the G_{LR} representations as

$$E_{10} \xrightarrow{M_{GUT}} D^{(10)}(3, 1, 1)_{-\frac{2}{3}} + \overline{D}^{(10)}(\overline{3}, 1, 1)_{\frac{2}{3}} + L_{LR}^{(10)}(1, 2, 2)_0, \tag{7}$$

$$E_{45} \xrightarrow{M_{GUT}} W_L^{(45)}(1, 3, 1)_0 + W_R^{(45)}(1, 1, 3)_0 + G^{(45)}(8, 1, 1)_0 + N^{(45)}(1, 1, 1)_0 + U^{(45)}(3, 1, 1)_{\frac{4}{3}} + \overline{U}^{(45)}(\overline{3}, 1, 1)_{-\frac{4}{3}} + Q_{LR}^{(45)}(3, 2, 2)_{-\frac{2}{3}} + \overline{Q}_{LR}^{(45)}(\overline{3}, 2, 2)_{\frac{2}{3}}. \tag{8}$$

⁶ See [20,21] for other possibilities.

Here and hereafter, the overline on the extra fields denotes a charge conjugation rather than a Dirac adjoint. By using the G_{LR} representations, Eq. (6) is decomposed as

$$\mathcal{L}_{\text{extra}} \supset y'_d Q_L H_L^* \overline{D}^{(10)} + y'_d L_R^c H_L^* L_{LR}^{(10)} + y'_d Q_R^c H_R D^{(10)} + y'_d L_L H_R L_{LR}^{(10)} + y'_u Q_L H_L \overline{U}^{(45)} + y'_u L_L H_L N^{(45)} + y'_u Q_R^c H_R^* U^{(45)} + y'_u L_R^c H_R^* N^{(45)}. \tag{9}$$

When we integrate out the extra particles, these contributions become the higher-dimensional operators which are summarized in Table 1. The resultant Yukawa coupling constants in the SM are proportional to M_R/M_{extra} , and hence, the top Yukawa coupling requires the extra particle masses should be around LR symmetry breaking scale.

Several comments of the above minimal setup is summarized as follows; see also [20,21].

- The large difference between the top mass and the other third generation one is the most serious problem in realization of the observed fermion masses in generic $SO(10)$ GUT models. This is not a matter in our model because there are two origins of the Yukawa interactions.
- Small difference between down-type quark masses and charged-lepton masses is introduced by higher-dimensional operators that come from $SO(10)$ breaking effects [25].
- The right-handed neutrino masses are around LR-breaking scale M_R . As we assume that the LR-breaking scale is around 10^{10} – 10^{12} GeV, the masses of the active neutrinos generated by the seesaw mechanism [4–8] tend to be much heavier than the observed ones. This is because the Dirac neutrino Yukawa coupling for the third generation is $O(1)$ since it is unified with the top Yukawa coupling.
- When we assume that large mixings in the MNS matrix are realized, the CKM matrix also should be a large mixing matrix because of the unification. However, this does not satisfy experimental results.

We can solve the above problems by cancellation between the contributions from the operators in Eq. (5) with some other higher-dimensional operators which include the GUT breaking effects. The latter operators are suppressed by a factor of $\langle H_{45} \rangle / \Lambda$. However, in this model, the suppression factor is not so small even if Λ is around the Planck scale, $M_{\text{Pl}} \sim 2.4 \times 10^{18}$ GeV, as $\langle H_{45} \rangle$ can be as large as around 10^{17} GeV. By the cancellation, the small neutrino Yukawa coupling can be achieved even for the $O(1)$ top Yukawa coupling, and hence the active neutrino masses satisfy the experimental results. The mixing matrices of the quarks and the neutrinos can also be consistent with each other by cancellation.

3 Gauge coupling unification

In the previous section, we introduce extra fermions to achieve the Yukawa interactions of the SM. In this section, we consider the renormalization group (RG) flow of the gauge couplings including the contributions of those extra matter multiplets as well as the $SU(2)_R$ doublet Higgs boson. We assume for simplicity that the masses of the extra fermions and $SU(2)_R$ doublet Higgs are M_R . As the extra fermions makes the gauge coupling constants become rather strong at around the GUT scale, it is important to take into account the two-loop contributions of the gauge coupling constants to the RG flow; see e.g. Refs. [26–28]. The extra Yukawa interactions to the two-loop RGE may slightly affect the precision of the unification and the GUT gauge-boson mass. Since those effects depend on the detailed mass spectrum of the extra fermions, we neglect those contributions in this paper.

The β function of the gauge coupling g_a is given by

$$\beta_{g_a} = \frac{1}{16\pi^2} a_a g_a^3 + \frac{1}{(16\pi^2)^2} b_{ab} g_a^3 g_b^2, \tag{10}$$

where a, b take values 1, 2, 3 which refer to $U(1)_Y, SU(2)_L$, and $SU(3)_C$ below M_R and take values 1, 2L, 2R, and 3 which refer to $U(1)_{B-L}, SU(2)_L, SU(2)_R$, and $SU(3)_C$ above M_R , respectively:

- Above M_R , the coefficients of the gauge coupling beta functions are

$$\begin{aligned} a_a &= (a_0)_a + N_E (a_{10})_a + N_E (a_{45})_a, \\ b_{ab} &= (b_0)_{ab} + N_E (b_{10})_{ab} + N_E (b_{45})_{ab}, \end{aligned} \tag{11}$$

where each of a_0 and b_0 contains contributions from the SM particles and the $SU(2)_R$ doublet Higgs; a_{10} and b_{10} from E_{10} ; a_{45} and b_{45} from E_{45} ; and N_E is the number of extra particle pairs. These coefficients above M_R are

given by⁷

$$\begin{aligned} (a_0)_a &= \begin{pmatrix} \frac{9}{2} \\ -\frac{19}{6} \\ -\frac{19}{6} \\ -7 \end{pmatrix}, & (a_{10})_a &= \begin{pmatrix} \frac{2}{3} \\ \frac{2}{3} \\ \frac{2}{3} \\ \frac{2}{3} \end{pmatrix}, \\ (a_{45})_a &= \begin{pmatrix} \frac{16}{3} \\ \frac{16}{3} \\ \frac{16}{3} \\ \frac{16}{3} \end{pmatrix}, & & \\ (b_0)_{ab} &= \begin{pmatrix} \frac{23}{4} & \frac{27}{4} & \frac{27}{4} & 4 \\ \frac{9}{4} & \frac{35}{6} & 0 & 12 \\ \frac{9}{4} & 0 & \frac{35}{6} & 12 \\ \frac{1}{2} & \frac{9}{2} & \frac{9}{2} & -26 \end{pmatrix}, \\ (b_{10})_{ab} &= \begin{pmatrix} \frac{1}{3} & 0 & 0 & \frac{8}{3} \\ 0 & \frac{49}{6} & \frac{3}{2} & 0 \\ 0 & \frac{3}{2} & \frac{49}{6} & 0 \\ \frac{1}{3} & 0 & 0 & \frac{38}{3} \end{pmatrix}, \\ (b_{45})_{ab} &= \begin{pmatrix} \frac{20}{3} & 6 & 6 & \frac{64}{3} \\ 2 & \frac{211}{3} & 9 & 16 \\ 2 & 9 & \frac{211}{3} & 16 \\ \frac{8}{3} & 6 & 6 & \frac{334}{3} \end{pmatrix}. \end{aligned} \tag{12}$$

We set the $SU(2)_L$ and $SU(2)_R$ gauge couplings equal, $g_{2L} = g_{2R} \equiv g_2$.

- Below M_R , on the other hand, they are given by

$$a_a = \begin{pmatrix} \frac{41}{10} \\ -\frac{19}{6} \\ -7 \end{pmatrix}, \quad b_{ab} = \begin{pmatrix} \frac{199}{50} & \frac{27}{10} & \frac{44}{5} \\ \frac{9}{10} & \frac{35}{6} & 12 \\ \frac{11}{10} & \frac{9}{2} & -26 \end{pmatrix}, \tag{14}$$

which come only from the SM particle contribution.

To calculate the RG flow for the gauge couplings, we consider the one-loop matching condition at the renormalization scale,

$$\begin{aligned} & \frac{1}{\alpha_1(M_R)} \Big|_{\text{Below}}^{M_R} \\ &= \frac{3}{5} \frac{1}{\alpha_{2R}(M_R)} + \frac{2}{5} \frac{1}{\alpha_1(M_R)} \Big|_{\text{Above}}^{M_R} - \frac{1}{2\pi} \frac{1}{10}. \end{aligned} \tag{15}$$

Recall that the value of gauge coupling for $SU(2)_R$ group is the same as that for the $SU(2)_L$ group above M_R : $\alpha_{2R} =$

⁷ There were minor errors in the two-loop coefficients in the first arXiv versions of our work and of Ref. [21]. The coefficients of the current version have been cross-checked by the authors of Ref. [21].

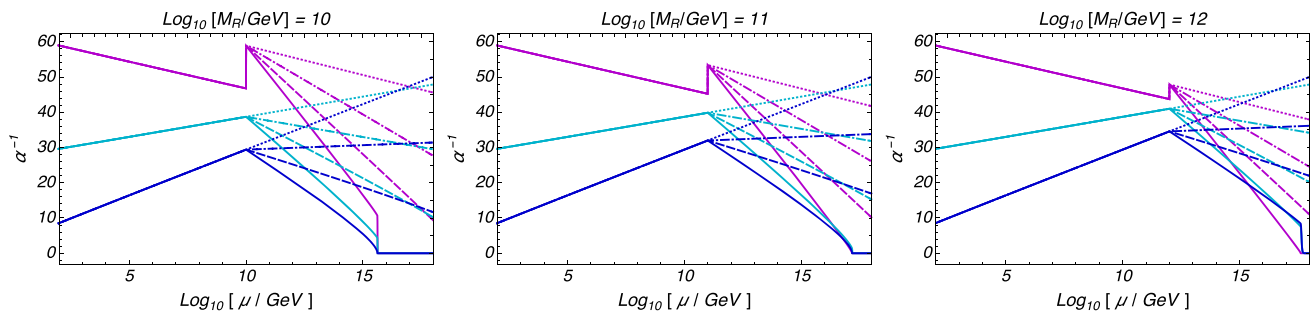


Fig. 1 The RG flow of the gauge couplings for $M_R = 10^{10}$ GeV, $M_R = 10^{11}$ GeV and $M_R = 10^{12}$ GeV form left to right. Below the LR symmetry breaking scale M_R , the purple, light-blue, and blue lines refer to gauge couplings of $U(1)_Y$, $SU(2)_L$, and $SU(3)_C$ gauge groups,

respectively. Above M_R , the purple line refers to the gauge coupling of the $U(1)_{B-L}$ group. $N_E = 3$ (solid), $N_E = 2$ (dashed), $N_E = 2$ (dashed-dotted), and $N_E = 0$ (dotted) pairs of the extra fermion are introduced

$\alpha_{2L} \equiv \alpha_2$. As we are taking the \overline{MS} renormalization scheme, there is a mass independent threshold correction in the right-hand side [29].⁸ In the following, we assume that the massive gauge boson of $SU(2)_R \times U(1)_{B-L}$ and the extra matter multiplets $E_{10,45}$ have the same mass of M_R for simplicity. The contributions of the extra matter do not affect the quality of the unification significantly as long as they have $SO(10)$ consistent masses.⁹

In Fig. 1, the RG flow of the gauge couplings is shown. The input values for the RG flow are taken to be the central values of the experimental measurements in [30]:

$$\begin{matrix} \alpha(M_W) & \alpha_3(M_Z) & \sin^2 \theta_W(M_Z) & M_Z[\text{GeV}] \\ 1/128 & 0.1181 & 0.23122 & 91.1876 \end{matrix} .$$

Below the LR symmetry breaking scale M_R , the purple, light-blue, and the blue lines refer to the gauge couplings for the $U(1)_Y$, the $SU(2)_L$, and the $SU(3)_C$ groups, respectively. Above M_R , the purple line refers to the gauge coupling for the $U(1)_{B-L}$ group. $N_E = 3$ (solid), $N_E = 2$ (dashed), $N_E = 1$ (dashed-dotted), and $N_E = 0$ (dotted) of the extra fermions are introduced. From the left to right, we take the LR symmetry breaking scale, $M_R = 10^{10}$ GeV, $M_R = 10^{11}$ GeV, and $M_R = 10^{12}$ GeV, respectively.

The figure shows that the gauge couplings of the LR symmetric model become close with each other at around $10^{17} - 10^{18}$ GeV for $M_R = 10^{10}$ GeV for $N_E \leq 2$. The three pairs of the extra multiplets at $M_R = 10^{10}$ GeV, on the other hand, lead to the Landau pole before unification. The gauge couplings for $M_R = 10^{11}$ GeV, on the other hand, meet well together before they hit the Landau pole. There, we see that the two-loop contributions are not negligible with which the

RG flow becomes non-linear. The results for $M_R = 10^{12}$ GeV also show that the gauge couplings become close with each other moderately at around $M_R = 10^{15}$ GeV.

To quantify the quality of the unification, let us consider the matching conditions between the gauge coupling constants in the LR symmetric model and the $SO(10)$ gauge coupling, $\alpha_G = g_G^2/4\pi$:

$$\begin{aligned} \frac{1}{\alpha_1(\mu, M_R)} &= \frac{1}{\alpha_G(\Lambda)} \\ &- \frac{1}{2\pi} \left(a_1 \log \frac{\mu}{\Lambda} - 14 \log \frac{M_X}{\Lambda} - 14 \log \frac{M_{X'}}{\Lambda} \right) \\ &- \frac{1}{2\pi} \frac{4}{3} + \frac{1}{2\pi} \Delta_1, \end{aligned} \tag{16}$$

$$\begin{aligned} \frac{1}{\alpha_2(\mu, M_R)} &= \frac{1}{\alpha_G(\Lambda)} \\ &- \frac{1}{2\pi} \left(a_2 \log \frac{\mu}{\Lambda} - 21 \log \frac{M_X}{\Lambda} \right) - \frac{1}{2\pi} + \frac{1}{2\pi} \Delta_2, \end{aligned} \tag{17}$$

$$\begin{aligned} \frac{1}{\alpha_3(\mu, M_R)} &= \frac{1}{\alpha_G(\Lambda)} \\ &- \frac{1}{2\pi} \left(a_3 \log \frac{\mu}{\Lambda} - 14 \log \frac{M_X}{\Lambda} - \frac{7}{2} \log \frac{M_{X'}}{\Lambda} \right) \\ &- \frac{1}{2\pi} \frac{5}{6} + \frac{1}{2\pi} \Delta_3. \end{aligned} \tag{18}$$

The parameters μ and Λ are the renormalization scale and the cutoff scale at around the GUT scale. The mass parameter M_X and $M_{X'}$ denotes the mass of the gauge boson in the $(3, 2, 2)_{-2/3}$ and $(3, 1, 1)_{-4/3}$ representations, respectively. For the symmetry breaking path $SO(10) \rightarrow SU(3) \times SU(2)_L \times SU(2)_R \times U(1)_{B-L}$ by the VEV of the Higgs boson in the 45 representation, it is predicted that $M_{X'} = 2M_X$. The mass independent threshold corrections are due to the \overline{MS} renormalization scheme, which are absent in the \overline{DR} renormalization scheme. The parameters $\Delta_{1,2,3}$ represent the threshold corrections from some particles at the GUT scale

⁸ For the \overline{DR} renormalization scheme, the mass independent threshold correction is absent.

⁹ The mass scales of the extra vector-like matter affect the size of the GUT gauge coupling constant. The mass splitting within the extra $SO(10)$ multiplets also affect the precision of the gauge coupling unification at the GUT scale.

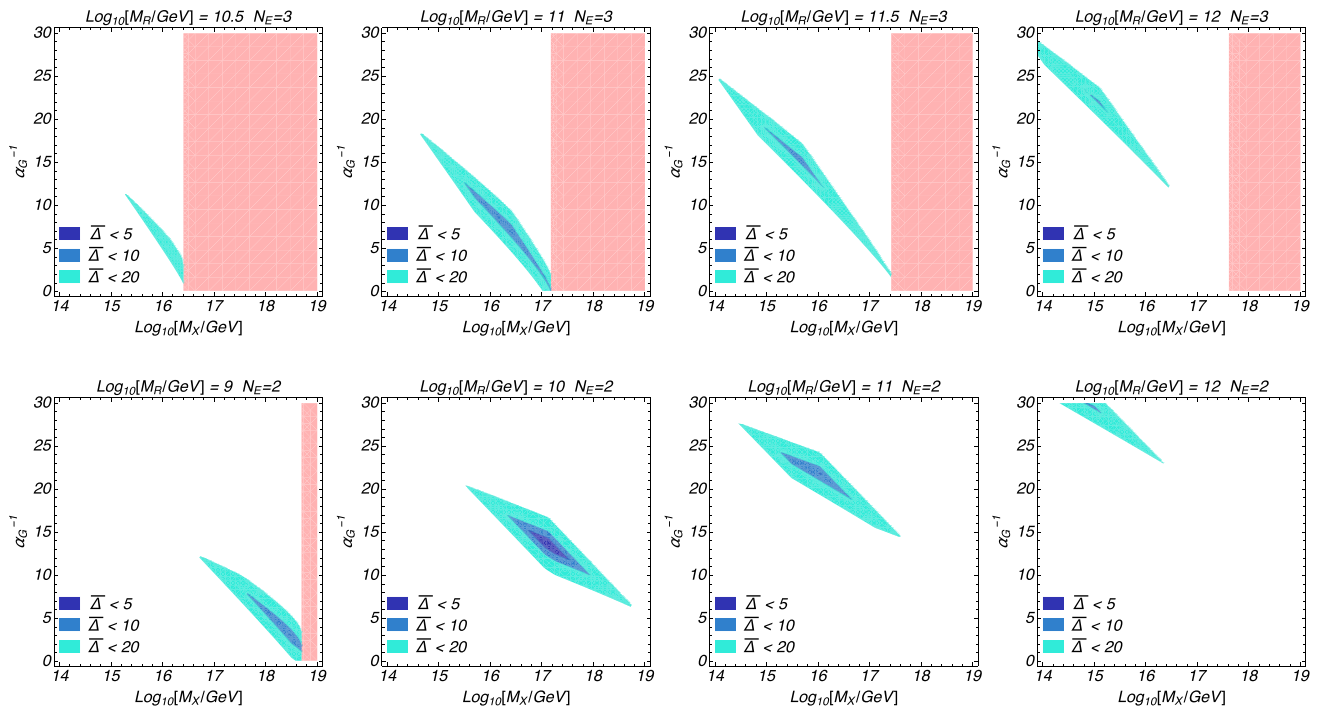


Fig. 2 The quality of the unification $\bar{\Delta}$ as a function of (M_X, α_G^{-1}) . The upper and the lower panels are for $N_E = 3$ and $N_E = 2$, respectively. The quality of the unification is reasonably high in the blue shaded region ($\bar{\Delta} < 5$), while it is moderate in the light-blue shaded region ($\bar{\Delta} < 10$). The parameter $\bar{\Delta}$ gets contribution not only from the

mass splittings of the GUT multiplets but also from the mass difference between the GUT particles and M_X . The pink shade region is excluded as M_X is above the Landau pole of $\alpha_{1,2,3}(\mu, M_R)$. We confine ourselves to the region with $M_X \ll M_{Pl}$, so that the effective field theory without gravity is valid

other than the GUT gauge bosons, although we do not specify them in this paper.¹⁰ See [20, 21] for various contributions of the GUT multiplets to $\Delta_{1,2,3}$.

As a measure of the quality of the unification, we define

$$\bar{\Delta} \equiv \max_{a=1,2,3} [\Delta_a], \tag{19}$$

where we take $\mu = \Lambda = M_X$. The definition of $\bar{\Delta}$ is different from the unification measure Δ defined in [20, 21]. The parameter $\bar{\Delta}$ gets a contribution not only from the mass splittings of the GUT multiplets but also from the mass difference between the GUT particles and M_X , while Δ in [20, 21] purely measures the precision of the unification.

In Fig. 2, we show $\bar{\Delta}$ as a function of (M_X, α_G^{-1}) for a given M_R . The quality of the unification is reasonably high in the blue shaded region ($\bar{\Delta} < 5$), while it is moderate in the light-blue shaded region ($\bar{\Delta} < 10$). The figure shows that a reasonable unification, i.e. $\bar{\Delta} < 5$, is not possible for $M_R = \mathcal{O}(10^{10})$ GeV due to the Landau pole for $N_E = 3$. The figure also shows that the unification is possible for a wide range of the GUT gauge-boson mass, $M_X = 10^{15}$ –

10^{17} GeV. These results should be compared with the previous analyses of the gauge coupling unification in the LR symmetric model which preferred $M_R = \mathcal{O}(10^{10})$ GeV and $M_X = \mathcal{O}(10^{17})$ GeV [17]. The difference of the results stem from the explicit inclusion of the three flavors of the extra multiplet into the analysis of the RG flow.

For comparison, we also show $\bar{\Delta}$ for $N_E = 2$. In this case, the Landau pole is at the very high energy scale and does not exclude the parameter region significantly. For $N_E = 2$, more precise unification is achieved for a lower M_R and a higher M_X than the case of $N_E = 3$. In such a parameter region, however, there is a tension with the possibility to obtain the first generation Yukawa couplings as the higher-dimensional operators suppressed by M_{GUT} .

4 Proton lifetime

In the present model, the exchanges of the massive gauge boson in the $(3, 2, 2)_{-2/3}$ representation, i.e. the X -type gauge bosons, induce the proton decay. Incidentally, the each of the $SU(2)_R$ doublet component of the X gauge boson belongs to the adjoint representation 24 and the anti-symmetric representation 10 of the minimal $SU(5)$ GUT

¹⁰ The parameters $\Delta_{1,2,3}$ also get contributions from higher-dimensional operators $\langle H_{45} \rangle / M_{Pl}$, although we assume that $\langle H_{45} \rangle / M_{Pl} \ll \mathcal{O}(1)$.

Table 2 The B and L violating operators mediated by the X gauge boson

G_{LR}	G_{SM}	$SU(3)_C \times U(1)_{em}$
$\mathcal{O}^{(1)} \equiv (\overline{L_L^c Q_L})(\overline{Q_R^c Q_R})$	$2(\overline{l_L^c q_L})(\overline{u_R^c d_R})$	$\mathcal{O}^1 \equiv 2(\overline{e_L^c u_L})(\overline{u_R^c d_R})$ $\mathcal{O}^2 \equiv 2(\overline{\nu_L^c d_L})(\overline{u_R^c d_R})$
$\mathcal{O}^{(2)} \equiv (\overline{L_R^c Q_R})(\overline{Q_L^c Q_L})$	$(\overline{e_R^c u_R})(\overline{q_L^c q_L})$	$\mathcal{O}^3 \equiv 2(\overline{e_R^c u_R})(\overline{u_L^c d_L})$

gauge symmetry, respectively. In general setup of the $SO(10)$ GUT, they have different masses (see e.g. [31]), while they are common in the LR symmetric model. The massive gauge boson in the $(3, 1, 1)_{4/3}$ representation, on the other hand, does not lead to the proton decay.

After integrating out the X gauge boson, the gauge interaction of the matter field F_{16} results in the B and L breaking operators $\mathcal{O}^{(1,2)}$ in Table 2. Those operators are reduced to

$$\mathcal{L}_{\text{eff}} = \frac{g_G^2}{M_X^2} \{ (\overline{e_R^c u_R})(\overline{q_L^c q_L}) + (\overline{l_L^c q_L})(\overline{u_R^c d_R}) \} + \frac{g_G^2}{M_X^2} (\overline{l_L^c q_L})(\overline{u_R^c d_R}), \quad (20)$$

in terms of the G_{SM} fields [32]; see also [33]. Below the electroweak symmetry breaking scale, we may decompose it into the proton decay operators in terms of the $SU(3)_C \times U(1)_{em}$ fields such that $\mathcal{L}_{\text{eff}} = C^I \mathcal{O}^I$ as in Table 2. In Eq. (20), we do not take account of the effects of the quark mixing angles [34].¹¹

The partial decay width for the $p \rightarrow \pi^0 e^+$ is given by

$$\Gamma(p \rightarrow \pi^0 e^+) \simeq \frac{m_p}{32\pi} \left\{ 1 - \left(\frac{m_{\pi^0}}{m_p} \right)^2 \right\}^2 \sum_{I=1,3} |C^I(m_p) W_0^I|^2, \quad (21)$$

where m_p and m_{π^0} are the proton and the neutral pion masses, respectively, and W_0^I are the proton form factor. We may safely approximate $\sum_{I=1,3} |C^I(m_p) W_0^I|^2 = \sum_{I=1,3} |C^I(m_p)|^2 W_0^2$. In this calculation, W_0 for the $p \rightarrow \pi^0 e^+$ decay mode is -0.131 GeV^2 , which has been obtained by a lattice simulation [37].

To calculate the coefficients of the proton decay operators at the proton mass scale m_p , we have to consider the

¹¹ In the present model, an SM fermion is a linear combination of the spinor F_{16} and the extra particles E_{10} and E_{45} [20,21], and therefore we should consider the proton decay operators which come from the gauge interactions of the extra particles too, strictly speaking. However, we have introduced the extra particles to realize the large Yukawa couplings, while the Yukawa couplings of the first two generations are small. Therefore, we expect that the contributions from extra particles are small for the first generation, and thus we do not consider a contribution from extra particles in this paper. The proton decay operators which come from the gauge interaction of the extra particle E_{10} are summarized in Refs. [35,36].

renormalization factor A . In this paper, we consider the one-loop level renormalization factor from gauge interactions. Here, we divide the energy region into two parts. The first region is between the GeV scale and the LR-breaking scale M_R , where the renormalization factor is written as A_{long} . The second region is between the LR-breaking scale M_R and the GUT scale M_{GUT} , where the renormalization factor is written as A_{short} . The total renormalization factor A is given by the product of these factors, $A = A_{\text{long}} \times A_{\text{short}}$. We calculate this renormalization factor for each of the proton decay operators $\mathcal{O}^{(1)}$ and $\mathcal{O}^{(2)}$.

The one-loop level renormalization factor for each gauge group is given by

$$A_a = \left(\frac{\alpha_a(M_{\text{start}})}{\alpha_a(M_{\text{end}})} \right)^{-\frac{C_a}{a_a}}, \quad (22)$$

where $M_{\text{end}} > M_{\text{start}}$; a_a is the coefficient for β function for each gauge coupling which are shown in Eqs. (11) and (14). C_a is the factor appearing in the anomalous dimension γ_a of the a th gauge interaction for an each proton decay operator:

$$\gamma_a = -2C_a \frac{g_a^2}{(4\pi)^2}. \quad (23)$$

The coefficient C_a is summarized in Ref. [38], with which the renormalization factors are given by¹²

$$A_{\text{long}}^{(1)} = \left(\frac{\alpha_3(1 \text{ GeV})}{\alpha_3(M_R)} \right)^{-2/a_3} \left(\frac{\alpha_2(M_Z)}{\alpha_2(M_R)} \right)^{-\frac{9}{4}/a_2} \left(\frac{\alpha_1(M_Z)}{\alpha_1(M_R)} \right)^{-\frac{11}{12}/a_1}, \quad (24)$$

$$A_{\text{long}}^{(2)} = \left(\frac{\alpha_3(1 \text{ GeV})}{\alpha_3(M_R)} \right)^{-2/a_3} \left(\frac{\alpha_2(M_Z)}{\alpha_2(M_R)} \right)^{-\frac{9}{4}/a_2} \left(\frac{\alpha_1(M_Z)}{\alpha_1(M_R)} \right)^{-\frac{23}{12}/a_1}, \quad (25)$$

$$A_{\text{short}}^{(1)} = A_{\text{short}}^{(2)} = \left(\frac{\alpha_3(M_R)}{\alpha_3(M_{\text{GUT}})} \right)^{-2/a_3} \left(\frac{\alpha_2(M_R)}{\alpha_2(M_{\text{GUT}})} \right)^{-2 \cdot \frac{9}{4}/a_2} \left(\frac{\alpha_1(M_R)}{\alpha_1(M_{\text{GUT}})} \right)^{-\frac{1}{4}/a_1}. \quad (26)$$

¹² We use the six flavor RG equations even below the electroweak scale. If we instead use the three flavor RG below the electroweak scale, the $A_{\text{long}}^{(1,2)}$ are slightly enhanced by about 10%.

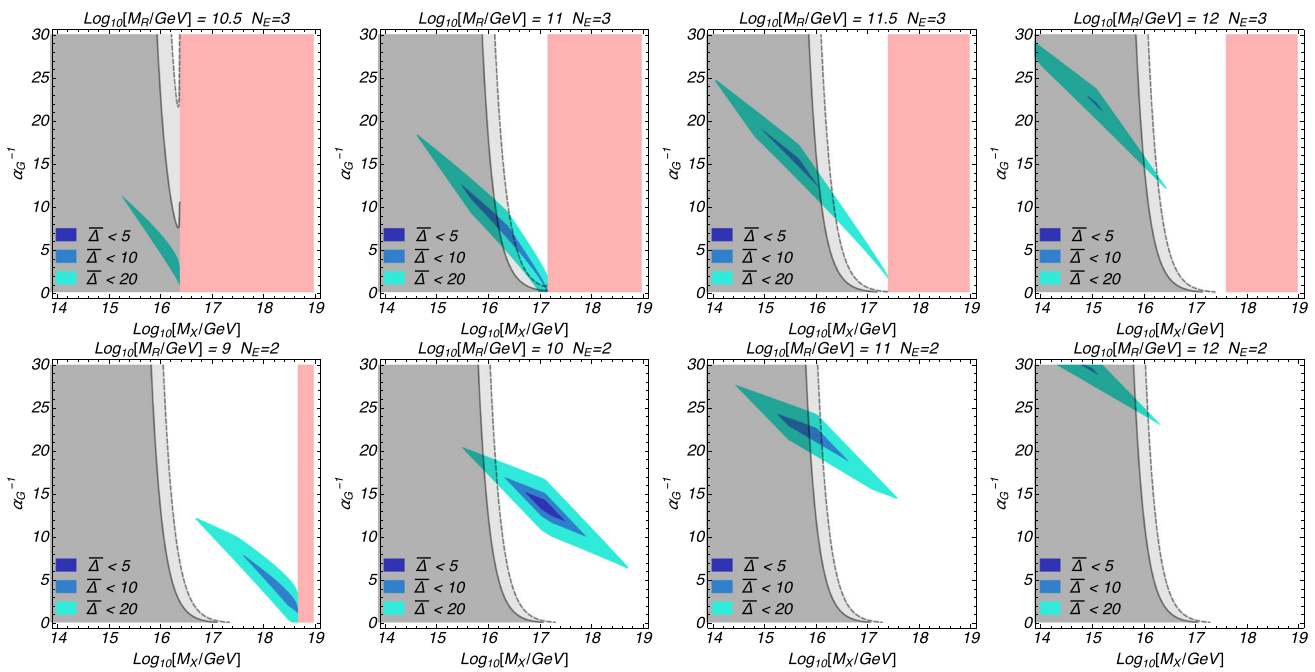


Fig. 3 The black solid and black dashed lines are proton decay constraints on the $p \rightarrow \pi^0 e^+$ decay mode from current SK limit and the future HK prospect. The gray shaded region is excluded by the current

SK limit and the region between black solid line and black dashed line will be explored by the HK experiment

In Eq. (26), we double the $SU(2)_L$ contribution to include the contribution from the $SU(2)_R$ gauge interaction. For $M_R \simeq 10^{11}$ GeV, $M_X \simeq 10^{16.5}$ GeV and $N_E = 3$, for example, we find that the renormalization factors are given by¹³

$$A^{(1)} = A_{\text{long}}^{(1)} A_{\text{short}}^{(1)} \simeq 5.9, \quad A^{(2)} = A_{\text{long}}^{(2)} A_{\text{short}}^{(2)} \simeq 6.0. \tag{27}$$

In Fig. 3, we overlay the current limit and the future prospects on the proton lifetime for $p \rightarrow \pi^0 e^+$ decay mode on Fig. 2. The current limit is the 90% CL exclusion limit by Super-kamiokande (SK) experiment, 1.6×10^{34} years [39], which is shown as the black solid line. The future prospects is the expected exclusion limit at 90% CL of the Hyper-K (HK) experiment, 1.3×10^{35} years [40], which is shown as the black dashed line. The figure shows that some part of the parameter region with moderate coupling unification has been excluded by the current SK limit for $M_R \gtrsim 10^{11.5}$ GeV ($N_E = 3$). The figure also shows that the HK experiment has a sufficient sensitivity to test large portion of the parameter space with moderate coupling unification for $M_R = O(10^{11})$ GeV for $N_E = 2, 3$.

5 Model with Peccei–Quinn symmetry

In the minimal setup with $N_E = 3$, we assume that all the SM Yukawa interactions are generated by integrating out the extra vector-like multiplets with masses around the LR-breaking scale. In this section, we briefly discuss a possibility to generate those masses by the PQ symmetry breaking. The PQ mechanism is one of the most successful solutions to the strong CP problem [41,42].¹⁴ There, the effective θ -angle of QCD is canceled by the VEV of the pseudo-Nambu–Goldstone boson, axion a , which is associated with the spontaneous breaking of the PQ symmetry [43,44]. The axion model not only solves the strong CP problem, but also provides a good candidate for cold dark matter [45–48]; see also Refs. [49–52]. In fact, the axion dark matter model is successful when the PQ breaking scale is of 10^{11} – 10^{12} GeV, which is close to the LR-breaking scale discussed in this paper; see [53] for review. This coincidence motivates us to see how it is successful to the mass scale of the extra vector-like fermions with the PQ breaking scale.

For this purpose, let us introduce a gauge singlet complex scalar field, P , which breaks the PQ symmetry at an intermediate scale. The PQ charge of P is defined to be 1. Below the PQ breaking scale, the axion appears as a phase component of P ,

¹³ For this choice, we find $\alpha_1^{-1}(M_X, M_R) \simeq 6.9$, $\alpha_2^{-1}(M_X, M_R) \simeq 7.3$, and $\alpha_3^{-1}(M_X, M_R) \simeq 6.0$, respectively.

¹⁴ Alternatively, the strong CP problem can be solved in the LR symmetric model by imposing space-time parity appropriately; see [20,21] and the references therein.

$$P = \frac{1}{\sqrt{2}} f_a e^{ia/f_a}, \tag{28}$$

where f_a is the decay constant of the axion. The PQ symmetry is realized by the shift of a ,

$$\frac{a}{f_a} \rightarrow \frac{a'}{f_a} = \frac{a}{f_a} + \alpha \quad (\alpha \in \mathbb{R}), \tag{29}$$

where the domain of the axion is given by $a/f_a = [-\pi, \pi)$.

To generate the extra fermion masses at the PQ scale, we assume that P couples to $E_{10,45}$ via,

$$\mathcal{L} = k_{10} P E_{10} E_{10} + k_{45} P E_{45} E_{45} + \text{h.c.}, \tag{30}$$

where $k_{10,45}$ are the coupling constants. Here, we assume that the PQ charges of E_{10} and E_{45} are $-1/2$. In this case, the interaction terms in Eq. (6) impose the requirement that the PQ charges of F_{16} are $1/2$, while that of H_{16} is vanishing.¹⁵

With these charge assignments, we find that the anomalous axion coupling to QCD is given by

$$\mathcal{L} = \frac{g_3^2}{32\pi^2} N_{\text{DW}} \frac{a}{f_a} G \tilde{G},$$

$$N_{\text{DW}} = (2N_{F_{16}} - N_{E_{10}} - 8N_{E_{45}}) = -21. \tag{31}$$

Here, G and \tilde{G} are the QCD field strength and its hodge dual, respectively. $N_{F_{16}} = 3$ is the number of generation of the SM fermions, and $N_{E_{10}} = N_{E_{45}} = N_E = 3$. The Lorentz and color indices are suppressed. Below the QCD scale the anomalous coupling of the axion to QCD in Eq. (31) leads to a non-vanishing axion potential and the axion settles down to its minimum which solves the strong CP problem.¹⁶ As both the extra fermions and the SM fermions possess the PQ charges, this model is in between the KSVZ [54,55] and DFSZ [56–58] invisible axion models, and is in principle distinguishable from these models.

The coherent oscillation of the axion turns into the dark matter density [59],

$$\Omega_a h^2 \simeq 0.18 \left(\frac{\Delta a_i}{F_{\text{eff}}} \right)^2 \left(\frac{F_{\text{eff}}}{10^{12} \text{ GeV}} \right)^{1.19}, \tag{32}$$

where we have defined $F_{\text{eff}} = f_a/N_{\text{DW}}$. $\Delta a_i/F_{\text{eff}} \in [-\pi, \pi)$ denotes the initial misalignment angle of the axion from the N_{DW} degenerate CP conserving vacua. Therefore, the axion dark matter scenario is successful for $F_{\text{eff}} \sim 10^{11-12}$ GeV for a typical initial misalignment angle. In this present model, the PQ breaking scale is given by $f_a = N_{\text{DW}} F_{\text{eff}}$, the axion dark

matter prefers the PQ breaking scale at $f_a \sim 10^{12-13}$ GeV. Accordingly, we find that the extra multiplet masses at $M_R \sim 10^{11}$ GeV can be provided for $k_{10,45} \sim 10^{-(1-2)}$ consistently with the axion dark matter scenario. It should be emphasized that this scenario does not work for $N_E = 2$ since the higher-dimensional operator to generate the SM Yukawa interactions of the first generation explicitly break the PQ symmetry.¹⁷

We argue that the axion in our setup is within the reach of future detection. Due to the non-vanishing axion potential, the axion gets a mass given by [60]

$$m_a \simeq 5.7 \mu\text{eV} \left(\frac{10^{12} \text{ GeV}}{F_{\text{eff}}} \right). \tag{33}$$

The axion also couples to photons through the electromagnetic anomaly N_{QED} and thorough the mixing with neutral mesons. Many on-going and future axion search experiments utilize the axion–photon coupling, which is parameterized as

$$\mathcal{L} \supset \frac{g_{a\gamma\gamma}}{4} a F \tilde{F}, \tag{34}$$

with [61]¹⁸

$$g_{a\gamma\gamma} = \frac{\alpha_{\text{EM}}}{2\pi F_{\text{eff}}} \left(\frac{N_{\text{QED}}}{N_{\text{DW}}} - 1.92(4) \right)$$

$$= \frac{\alpha_{\text{EM}}}{2\pi F_{\text{eff}}} \left(\frac{8}{3} - 1.92(4) \right). \tag{35}$$

Note that $g_{a\gamma\gamma}$ in our model is equivalent to that in the DFSZ axion model [56–58], which is already excluded by the current ADMX experiment for $m_a \simeq 2.7\text{--}3.3 \mu\text{eV}$ [62,63]. The higher mass range of m_a up to $400 \mu\text{eV}$ (corresponding to $F_{\text{eff}} \sim 10^{11}$ GeV) is expected to be covered by future cavity haloscopes such as ADMX [62], CULTASK [64] and MAD-MAX [65]; see also Ref. [66,67].

Several comments are in order. The axion potential induced by the anomalous QCD coupling in Eq. (31) possesses $\mathbb{Z}_{N_{\text{DW}}}$ discrete symmetry in the domain of the axion $a/f_a \in [-\pi, \pi)$, or equivalently in $a/F_{\text{eff}} \in N_{\text{DW}} \times [-\pi, \pi)$. The discrete symmetry is spontaneously broken by the VEV of the axion. Thus, the domain wall formation takes place after the onset of the coherent oscillation of the axion, if the initial misalignment angle in each Hubble volume of the Universe at that time is random. Once the domain walls are formed, they immediately dominate the Universe, which conflicts with the Standard Cosmology. To avoid this problem, we need to assume that the PQ symmetry breaking takes place before inflation and never gets restored after inflation. Under this assumption, the initial misalignment angle of the axion is uniform in the entire Universe, and hence the axion

¹⁵ We may consider a model in which E_{10} and E_{45} have the opposite PQ charges. In this case the PQ charge of F_{16} is vanishing, although the domain wall number is again $N_{\text{DW}} = -21$.

¹⁶ Here, the origin of the axion field space is taken to be the one at which the effective θ -angle of QCD is vanishing without loss of generality.

¹⁷ We may consider the PQ symmetry which is spontaneously broken at the cutoff scale even for $N_E = 2$. In such a case, however, the axion dark matter scenario is not successful.

¹⁸ The ratio $N_{\text{QED}}/N_{\text{DW}} = 8/3$ is a generic feature of the GUT consistent PQ charge assignment.

sits in the same sub-domain and evades the formation of the domain wall.

We mention that the large domain wall number, $N_{\text{DW}} = -21$, is advantageous to avoid the PQ symmetry restoration, since the actual PQ breaking scale is an order of magnitude larger than the effective decay constant F_{eff} appropriate for the axion dark matter scenario, i.e. $F_{\text{eff}} \sim 10^{11-12}$ GeV. Therefore, the present model can be consistent with a cosmological scenario with higher reheating temperature than in the conventional axion dark matter models. In this sense, the present model can be more easily consistent with the thermal leptogenesis scenario [68] which requires a rather high reheating temperature, $T_R \gtrsim 10^{9-10}$ GeV [69–71].¹⁹

As another comment, the massless axion fluctuates quantum mechanically during inflation, which leads to the isocurvature fluctuation of the axion dark matter density when the PQ symmetry breaking takes place before inflation. The dark matter isocurvature fluctuation have been severely constrained by the precise measurements of the cosmic microwave background [75]. The amplitude of the isocurvature fluctuation is proportional to the Hubble parameter during inflation, H_I . As a result, H_I is constrained from above as $H_I \lesssim 10^{7-8}$ GeV to avoid the current constraint; see e.g. Refs. [53, 76]. Therefore, the present scenario with the axion dark matter can be refuted if the primordial B -mode polarization in the cosmic microwave background is discovered in near future; see, e.g. Refs. [77–79].

Finally, let us comment on the origin of the PQ symmetry. By definition, the $U(1)$ PQ symmetry cannot be an exact symmetry as it is explicitly broken by the QCD anomaly. Besides, it is also argued that any global symmetries are broken by quantum gravity effects [78–84]. When explicit breaking terms exist, the effective θ angle of QCD is non-vanishing even in the presence of the axion, which spoils the PQ mechanism. For example, if the PQ symmetry is completely broken by the quantum gravity effects, it is expected that there should be a PQ breaking term at least,

$$\mathcal{L}_{\text{PQ breaking}} = \frac{P^5}{M_{\text{Pl}}} + \text{h.c.}, \quad (36)$$

which drastically affects the axion potential and spoils the PQ mechanism.

In the present model, however, we may regard that the discrete $\mathbb{Z}_{2N_{\text{DW}}}$ symmetry to be a discrete gauge symmetry as it

can satisfy the anomaly free conditions [85].²⁰ If $\mathbb{Z}_{2N_{\text{DW}}}$ symmetry is a gauge symmetry, the lowest-dimensional operator which breaks the $U(1)$ PQ symmetry but is invariant under the $\mathbb{Z}_{2N_{\text{DW}}}$ gauge symmetry is given by

$$\mathcal{L}_{\text{PQ breaking}} = \frac{P^{21}}{M_{\text{Pl}}^{17}} + \text{h.c.}, \quad (37)$$

which is highly suppressed and does not spoil the PQ mechanism; see e.g. Ref. [86]. This argument strengthens the PQ mechanism in the present model.²¹

6 Summary

In this paper, we have investigated the proton lifetime in the $SO(10)$ GUT which is broken down by the VEV of H_{45} to the minimal LR symmetric gauge group $SU(3)_C \times SU(2)_L \times SU(2)_R \times U(1)_Y$, which is in turn broken at the intermediate LR-breaking scale M_R by the $SU(2)_R$ doublet Higgs that is a part of H_{16} . The $SU(2)_L$ doublet component of the same H_{16} field eventually plays the role of the SM Higgs doublet. Due to the absence of the bi-doublet Higgs boson, the LR-breaking scale is determined to be at around 10^{10-12} GeV in order to achieve the gauge coupling unification.

As a notable feature of the model, it requires extra vector-like fermions to generate the SM Yukawa interactions. Such extra multiplets affect the RG flow, and lower the unification scale down to $M_X \lesssim 10^{17}$ GeV from that expected in Refs. [16, 17] by a factor a few or so. We have also found that the Wilson coefficients of the proton decay operators are considerably larger than those in the minimal $SU(5)$ GUT model. As a result, the proton decay rate is enhanced and we find that some portion of the parameter space consistent with the gauge coupling unification can be tested by the Hyper-K experiment thorough the proton decay search even when the GUT gauge-boson mass is in the range 10^{16-17} GeV.

We also discussed a possibility to generate the mass of the extra vector-like multiplets by the PQ symmetry breaking. We found that the axion dark matter scenario and the present model can be successfully combined for the model with $N_E = 3$. This combination can be tested by the proton decay search, the axion search and the search for the primordial B -mode fluctuation in the cosmic microwave background.

²⁰ Here, we normalize the charges of the discrete symmetry so that the extra vector-like multiplets have a charge -1 . Accordingly, the PQ breaking field P possesses the discrete charge 2.

²¹ We discuss the domain wall problem in Appendix A. As another possible justification of the $U(1)$ PQ symmetry, we may consider a $U(1)$ gauge symmetry with an accidental global $U(1)$ PQ symmetry [87], where E_{10} and E_{45} couple to a different PQ charged complex scalars; see Refs. [88–90] for details.

¹⁹ For a given reheating temperature T_R , the maximal temperature of the Universe of the thermal plasma during the inflaton dominated era is in general much higher than T_R up to $T_{\text{Max}} \sim (T_R^2 H_I M_{\text{Pl}})^{1/4}$ [72–74]. Here, H_I is the Hubble parameter during inflation and M_{Pl} is the reduced Planck scale.

Acknowledgements We thank Shigeki Matsumoto, Kyohei Mukaida, and Kenichi Saikawa for useful discussion. We are grateful to Keisuke Harigaya for valuable comments and cross-checks. This work is supported in part by JSPS KAKENHI Grant nos. 15H05889, 16H03991, 17H02878, 18H05542 (M.I.), 19H01899 (K.O.) 15H05889, 15K21733, and 17H02875 (N.Y.); World Premier International Research Center Initiative (WPI Initiative), MEXT, Japan (M.I.); National Natural Science Foundation of China (NNSFC) under Contracts Nos. 11675061, 11775092, 11521064, and 11435003 (Y.M.); and the European Union via the Advanced ERC grant SM-grav, No 669288 (Y.H.).

Data Availability Statement This manuscript has no associated data or the data will not be deposited. [Authors' comment: This is a theoretical study and no experimental data has been listed.]

Open Access This article is licensed under a Creative Commons Attribution 4.0 International License, which permits use, sharing, adaptation, distribution and reproduction in any medium or format, as long as you give appropriate credit to the original author(s) and the source, provide a link to the Creative Commons licence, and indicate if changes were made. The images or other third party material in this article are included in the article's Creative Commons licence, unless indicated otherwise in a credit line to the material. If material is not included in the article's Creative Commons licence and your intended use is not permitted by statutory regulation or exceeds the permitted use, you will need to obtain permission directly from the copyright holder. To view a copy of this licence, visit <http://creativecommons.org/licenses/by/4.0/>. Funded by SCOAP³.

Appendix

A Discrete gauge symmetry and the domain wall problem

In Sect. 5, we considered a discrete gauge symmetry which explains the origin of the approximate global $U(1)$ PQ symmetry. In this appendix, we briefly comment on the domain wall problem in the presence of the discrete gauge symmetry behind the PQ symmetry. In this set up, the N_{DW} axion domains in $a/F_{\text{eff}} = N_{\text{DW}} \times [-\pi, \pi)$ are gauge equivalent with each other, and hence, the axion domain wall configurations which connect different domains are not completely stable. As we will see, however, the axion domain wall problem remains even in the model with the discrete gauge symmetry.

To make our discussion concrete, let us assume that the discrete $\mathbb{Z}_{N_{\text{DW}}}$ gauge symmetry originates from a $U(1)$ gauge symmetry broken by the VEV of a complex scalar Φ whose gauge charge is large, $N_{\text{DW}} \gg 1$. Note that this $U(1)$ gauge symmetry is different from the global $U(1)$ PQ symmetry. The $U(1)$ gauge charge of the PQ breaking field P is 1 as

in Sect. 5.²² The VEV of the PQ breaking field P eventually breaks the $\mathbb{Z}_{N_{\text{DW}}}$ symmetry.

In this model, the stable topological defect is not the domain wall but the local strings which are associated with the spontaneous $U(1)$ gauge symmetry breaking. For example, a cosmic local string around which the phase of Φ winds from $0-2\pi$ are expected to be formed when Φ obtains a VEV at a very high energy scale. The phase of the PQ breaking field P is changed by $2\pi/N_{\text{DW}}$ under the parallel transport around this local string, which corresponds to the Aharonov–Bohm effect.

Now let us assume that the spontaneous symmetry breaking of the $U(1)$ gauge symmetry by the VEV of Φ takes place well before inflation, while the approximate global PQ symmetry breaking occurs after inflation. In this case, the cosmic local strings that are formed when Φ obtains a VEV have been diluted away by cosmic inflation. After inflation, the cosmic temperature decreases below the PQ breaking scale. Then, associated with the spontaneous breaking of the approximate global $U(1)$ PQ symmetry, a few cosmic global strings are expected to be formed in each Hubble volume. Note that these global strings are different from the ones diluted away during the inflation. When we turn around the global string, the phase of the PQ field P takes values from 0 to 2π when the winding number is one, and hence, the axion field takes values from 0 to $f_a \times 2\pi = N_{\text{DW}} \times F_{\text{eff}} \times 2\pi$.

Around the global string, the $[0, N_{\text{DW}} \times F_{\text{eff}} \times 2\pi)$ region has N_{DW} domains that are gauge equivalent under the $\mathbb{Z}_{N_{\text{DW}}}$. Since the approximate $U(1)$ PQ symmetry is highly protected by the $\mathbb{Z}_{N_{\text{DW}}}$ symmetry, the tension of the domain walls connecting the N_{DW} domains is negligibly small. Therefore, we have no domain wall problem associated with the $\mathbb{Z}_{N_{\text{DW}}}$ symmetry breaking by $\langle P \rangle \neq 0$. When the cosmic temperature decreases further, the cosmic global string networks follow the so-called scaling solution where the number of the cosmic global strings in each Hubble volume at that time remains of $\mathcal{O}(1)$; see e.g. [91]. When the axion potential is generated at around the QCD scale Λ_{QCD} , potential barriers appear around each global string, which results in N_{DW} domain walls whose boundaries are global strings.

As mentioned earlier, each domain wall attached to the global string connects different domains which are gauge equivalent under the discrete $\mathbb{Z}_{N_{\text{DW}}}$ symmetry. Therefore, this domain wall is not completely stable. In fact, each wall can be punctured by a loop of the earlier mentioned local string, around which the phase of Φ winds from 0 to 2π , since this local string connects the different axion domains without

²² To make the $U(1)$ gauge symmetry anomaly free, we need to introduce additional SM charged fermions (see e.g. [88–90]), although they do not affect the following discussion. Here, we only pay attention to the complex scalars where $\mathbb{Z}_{N_{\text{DW}}}$ instead of $\mathbb{Z}_{2N_{\text{DW}}}$ is good enough for the following discussion.

potential barrier. Once the domain wall is punctured, the loop of local string expands on the domain wall, and the domain wall disappears eventually. The rate of such a puncturing process, however, is highly suppressed, since the formation of the loop of the local string is suppressed by $e^{-|\langle\Phi\rangle|^4/\Lambda_{\text{QCD}}^2 F_{\text{eff}} T}$ at a temperature below the QCD scale: $T \lesssim \Lambda_{\text{QCD}}$.²³ As a result, the domain walls are virtually stable below the QCD scale and they immediately dominate over the energy density of the Universe, which causes the domain wall problem.²⁴

References

1. H. Georgi, S.L. Glashow, Phys. Rev. Lett. **32**, 438 (1974)
2. H. Georgi, AIP. Conf. Proc. **23**, 575 (1975)
3. H. Fritzsch, P. Minkowski, Ann. Phys. **93**, 193 (1975)
4. P. Minkowski, Phys. Lett. B **67**, 421 (1977)
5. T. Yanagida, in *Proceedings of the Workshop on Unified Theory and Baryon Number of the Universe*, ed. by O. Sawada, A. Sugamoto (KEK, 1979) p. 95
6. M. Gell-Mann, P. Ramond, R. Slansky, in *Supergravity*, ed. by P. van Nieuwenhuizen, D. Freedman (North Holland, Amsterdam, 1979)
7. S.L. Glashow, in *Proceedings of the Cargèse Summer Institute on Quarks and Leptons*, ed. by M. Lévy et al. Cargèse, July 9–29, 1979, (Plenum, New York, 1980), p. 707
8. R.N. Mohapatra, G. Senjanovic, Phys. Rev. Lett. **44**, 912 (1980)
9. J.C. Pati, A. Salam, Phys. Rev. D **10**, 275 (1974). (**Erratum: [Phys. Rev. D **11**, 703 (1975)]**)
10. R.N. Mohapatra, J.C. Pati, Phys. Rev. D **11**, 566 (1975)
11. R.N. Mohapatra, J.C. Pati, Phys. Rev. D **11**, 2558 (1975)
12. G. Senjanovic, R.N. Mohapatra, Phys. Rev. D **12**, 1502 (1975)
13. R.N. Mohapatra, F.E. Paige, D.P. Sidhu, Phys. Rev. D **17**, 2462 (1978)
14. G. Senjanovic, Nucl. Phys. B **153**, 334 (1979)
15. R.N. Mohapatra, R.E. Marshak, Phys. Rev. Lett. **44**, 1316 (1980). (**Erratum: [Phys. Rev. Lett. **44**, 1643 (1980)]**)
16. D. Chang, R.N. Mohapatra, J. Gipson, R.E. Marshak, M.K. Parida, Phys. Rev. D **31**, 1718 (1985)
17. F. Siringo, Phys. Part. Nucl. Lett. **10**(2), 94 (2013)
18. S. Rajpoot, Phys. Rev. D **22**, 2244 (1980)
19. M. Fukugita, T. Yanagida, (Springer, Berlin, 2003)
20. L.J. Hall, K. Harigaya, JHEP **1810**, 130 (2018)
21. L.J. Hall, K. Harigaya, JHEP **1911**, 033 (2019)
22. Y. Hamada, M. Ibe, S. Matsumoto, K. Mukaida, K. Oda, K. Saikawa, N. Yokozaki, “*LR-UNIFICATION*,” *YITP Workshop on “LHC vs Beyond the Standard Model—Frontier of particle physics,”* 19–25 March 2013, Yukawa Institute, Japan
23. S. Bertolini, L. Di Luzio, M. Malinsky, Phys. Rev. D **80**, 015013 (2009)
24. S. Bertolini, L. Di Luzio, M. Malinsky, Phys. Rev. D **81**, 035015 (2010)
25. J.R. Ellis, M.K. Gaillard, Phys. Lett. B **88**, 315 (1979)
26. D.R.T. Jones, Phys. Rev. D **25**, 581 (1982)
27. M.E. Machacek, M.T. Vaughn, Nucl. Phys. B **222**, 83 (1983)
28. H. Arason, D.J. Castano, B. Keszthelyi, S. Mikaelian, E.J. Piard, P. Ramond, B.D. Wright, Phys. Rev. D **46**, 3945 (1992)
29. S. Weinberg, Phys. Lett. B **91**, 51 (1980)
30. M. Tanabashi et al. [Particle Data Group], Phys. Rev. D **98**(3), 030001 (2018)
31. N. Haba, Y. Mimura, T. Yamada, JHEP **1907**, 155 (2019)
32. S. Bertolini, L. Di Luzio, M. Malinsky, Phys. Rev. D **87**(8), 085020 (2013)
33. P. Langacker, Phys. Rep. **72**, 185 (1981)
34. J.R. Ellis, M.K. Gaillard, D.V. Nanopoulos, S. Rudaz, Nucl. Phys. B **176**, 61 (1980)
35. N. Maekawa, Y. Muramatsu, Phys. Rev. D **88**(9), 095008 (2013)
36. N. Maekawa, Y. Muramatsu, Phys. Lett. B **767**, 398 (2017)
37. Y. Aoki, T. Izubuchi, E. Shintani, A. Soni, Phys. Rev. D **96**(1), 014506 (2017)
38. W.E. Caswell, J. Milutinovic, G. Senjanovic, Phys. Rev. D **26**, 161 (1982)
39. K. Abe et al. [Super-Kamiokande Collaboration], Phys. Rev. D **95**(1), 012004 (2017)
40. K. Abe et al., [arXiv:1109.3262](https://arxiv.org/abs/1109.3262) [hep-ex]
41. R.D. Peccei, H.R. Quinn, Phys. Rev. Lett. **38**, 1440 (1977)
42. R.D. Peccei, H.R. Quinn, Phys. Rev. D **16**, 1791 (1977)
43. S. Weinberg, Phys. Rev. Lett. **40**, 223 (1978)
44. F. Wilczek, Phys. Rev. Lett. **40**, 279 (1978)
45. M. Dine, W. Fischler, Phys. Lett. B **120**, 137 (1983)
46. L.F. Abbott, P. Sikivie, Phys. Lett. B **120**, 133 (1983)
47. J. Preskill, M.B. Wise, F. Wilczek, Phys. Lett. B **120**, 127 (1983)
48. J. Preskill, S.P. Trivedi, F. Wilczek, M.B. Wise, Nucl. Phys. B **363**, 207 (1991)
49. M.I. Vysotsky, Y.B. Zeldovich, M.Y. Khlopov, V.M. Chechetkin, Pisma. Zh. Eksp. Teor. Fiz. **27**, 533 (1978)
50. M.I. Vysotsky, Y.B. Zeldovich, M.Y. Khlopov, V.M. Chechetkin, JETP Lett. **27**, 502 (1978)
51. Z.G. Berezhiani, A.S. Sakharov, M.Y. Khlopov, Sov. J. Nucl. Phys. **55**, 1063 (1992)
52. Z.G. Berezhiani, A.S. Sakharov, M.Y. Khlopov, Yad. Fiz. **55**, 1918 (1992)
53. M. Kawasaki, K. Nakayama, Ann. Rev. Nucl. Part. Sci. **63**, 69 (2013)
54. J.E. Kim, Phys. Rev. Lett. **43**, 103 (1979)
55. M.A. Shifman, A.I. Vainshtein, V.I. Zakharov, Nucl. Phys. B **166**, 493 (1980)
56. A.R. Zhitnitsky, Sov. J. Nucl. Phys. **31**, 260 (1980)
57. A.R. Zhitnitsky, Yad. Fiz. **31**, 497 (1980)
58. M. Dine, W. Fischler, M. Srednicki, Phys. Lett. B **104**, 199 (1981)
59. M.S. Turner, Phys. Rev. D **33**, 889 (1986)
60. M. Gorghetto, G. Villadoro, JHEP **1903**, 033 (2019)
61. G.G. di Cortona, E. Hardy, J.P. Vega, G. Villadoro, JHEP **1601**, 034 (2016)
62. N. Du et al. [ADMX Collaboration], Phys. Rev. Lett. **120**(15), 151301 (2018)
63. T. Braine et al. [ADMX Collaboration]. [arXiv:1910.08638](https://arxiv.org/abs/1910.08638) [hep-ex]
64. E. Petrakou [CAPP/IBS Collaboration], EPJ Web Conf. **164**, 01012 (2017)
65. A. Caldwell et al. [MADMAX Working Group], Phys. Rev. Lett. **118**(9), 091801 (2017)
66. P.W. Graham, I.G. Irastorza, S.K. Lamoreaux, A. Lindner, K.A. van Bibber, Ann. Rev. Nucl. Part. Sci. **65**, 485 (2015)
67. M. Lawson, A.J. Millar, M. Pancaldi, E. Vitagliano, F. Wilczek, Phys. Rev. Lett. **123**(14), 141802 (2019)
68. M. Fukugita, T. Yanagida, Phys. Lett. B **174**, 45 (1986)
69. G.F. Giudice, A. Notari, M. Raidal, A. Riotto, A. Strumia, Nucl. Phys. B **685**, 89 (2004)

²³ For a loop of a radius ℓ , the removed wall energy is $\sim \ell^2 \times m_a F_{\text{eff}}^2$, while the string energy cost is $\sim \ell \times |\langle\Phi\rangle|^2$. Therefore we need at least $\ell \gtrsim |\langle\Phi\rangle|^2 / m_a F_{\text{eff}}^2$. Multiplying the string tension $|\langle\Phi\rangle|^2$ and putting $m_a \sim \Lambda_{\text{QCD}}^2 / F_{\text{eff}}$, the lowest mass of the string loop which can puncture the domain wall is $|\langle\Phi\rangle|^4 / \Lambda_{\text{QCD}}^2 F_{\text{eff}}$.

²⁴ For a study of cosmic string formation when both Φ and P obtain VEVs after inflation, see Ref. [92].

70. W. Buchmuller, R.D. Peccei, T. Yanagida, *Ann. Rev. Nucl. Part. Sci.* **55**, 311 (2005)
71. S. Davidson, E. Nardi, Y. Nir, *Phys. Rep.* **466**, 105 (2008)
72. E.W. Kolb, M.S. Turner, *Front. Phys.* **69**, 1 (1990)
73. J. Yokoyama, *Phys. Rev. D* **70**, 103511 (2004)
74. K. Harigaya, K. Mukaida, *JHEP* **1405**, 006 (2014)
75. Y. Akrami et al. [Planck Collaboration], [arXiv:1807.06211](https://arxiv.org/abs/1807.06211) [astro-ph.CO]
76. M. Kawasaki, E. Sonomoto, T.T. Yanagida, *Phys. Lett. B* **782**, 181 (2018)
77. K.N. Abazajian et al. [CMB-S4 Collaboration], [arXiv:1610.02743](https://arxiv.org/abs/1610.02743) [astro-ph.CO]
78. G.V. Lavrelashvili, V.A. Rubakov, P.G. Tinyakov, *JETP Lett.* **46**, 167 (1987)
79. G.V. Lavrelashvili, V.A. Rubakov, P.G. Tinyakov, *Pisma. Zh. Eksp. Teor. Fiz.* **46**, 134 (1987)
80. S.W. Hawking, *Phys. Lett. B* **195**, 337 (1987)
81. S.B. Giddings, A. Strominger, *Nucl. Phys. B* **307**, 854 (1988)
82. S.R. Coleman, *Nucl. Phys. B* **310**, 643 (1988)
83. G. Gilbert, *Nucl. Phys. B* **328**, 159 (1989)
84. T. Banks, N. Seiberg, *Phys. Rev. D* **83**, 084019 (2011)
85. C. Csaki, H. Murayama, *Nucl. Phys. B* **515**, 114 (1998)
86. L.M. Carpenter, M. Dine, G. Festuccia, *Phys. Rev. D* **80**, 125017 (2009)
87. S.M. Barr, D. Seckel, *Phys. Rev. D* **46**, 539 (1992)
88. H. Fukuda, M. Ibe, M. Suzuki, T.T. Yanagida, *Phys. Lett. B* **771**, 327 (2017)
89. H. Fukuda, M. Ibe, M. Suzuki, T.T. Yanagida, *JHEP* **1807**, 128 (2018)
90. M. Ibe, M. Suzuki, T.T. Yanagida, *JHEP* **1808**, 049 (2018)
91. A. Vilenkin, E.P.S. Shellard, *Cosmic Strings and Other Topological Defects* (Cambridge University Press, 2000)
92. T. Hiramatsu, M. Ibe, M. Suzuki, [arXiv:1910.14321](https://arxiv.org/abs/1910.14321) [hep-ph]